Geosciences **2015**, *5*, 30-44; doi:10.3390/geosciences5010030

OPEN ACCESS

geosciences

ISSN 2076-3263

www.mdpi.com/journal/geosciences

Communication

Probing the Hidden Geology of Isidis Planitia (Mars) with Impact Craters

Graziella Caprarelli [1,*] and Roberto Orosei [2]

[1] Division of IT, Engineering and the Environment, University of South Australia, GPO Box 2471, Adelaide, SA 5001, Australia

[2] Istituto di Radioastronomia, Istituto Nazionale di Astrofisica, Via Piero Gobetti 101, 40129 Bologna, Italy; E-Mail: roberto.orosei@inaf.it

* Author to whom correspondence should be addressed; E-Mail: graziella.caprarelli@unisa.edu.au; Tel./Fax: +61-8-830-21870.

Academic Editor: Jesus Martinez-Frias

Received: 31 December 2014 / Accepted: 5 February 2015 / Published: 13 February 2015

Abstract: In this study we investigated Isidis Planitia, a 1325 km diameter multi-ring impact basin intersecting the Martian hemispheric dichotomy, located in the eastern hemisphere, between Syrtis Major and Utopia Planitia. From Mars Orbiter Laser Altimeter gridded data we observed that in the center of Isidis the −3700 m and −3800 m isolines strike NW-SE, being quasi-parallel to the diameter of the basin. We interpreted this as evidence that the basement of Isidis Planitia was faulted prior to being completely covered by layers of sediments and volcanic rocks. Plotting the morphometric data of impact craters located on the floor of the basin in a measured depths *vs.* predicted depths diagram (MPD), we concluded that the fault planes should dip SW, which is consistent with the location of the most topographically depressed sector of Isidis Planitia. We also estimated a minimum vertical displacement of ~1–2 km. Considering that the crust under Isidis Planitia is only a few km thick, our estimate implies brittle behavior of the lithosphere under the basin, suggesting that a low geothermal gradient and rheologically strong material characterize this Martian location.

Keywords: Mars; Isidis Planitia; MOLA DEM; impact craters; tectonics; lithosphere

---

1. Introduction

Isidis Planitia occupies the interior of a multi-ringed impact crater [1,2] located in the eastern hemisphere of Mars along the crustal dichotomy (Figure 1). It is separated from the expanse of the northern hemispheric plains by an elevation saddle beyond which the Utopia Planitia basin is observed to slope S-N by an angle of ~0.036°, which is a global feature of the Martian northern lowlands [3]. Even though the material inside Isidis is geomorphologically part of the northern lowlands, as shown in geological [4,5] and fractal behavior [6] maps, its floor gently dips SW by an angle of ~0.02° [7]. A flexural model suggests this may be due to a 6 km deflection in Utopia Planitia caused by sediment load generating a peripheral bulge, of which the floor of Isidis Planitia represents the southwestern limb [8]. Combining Mars Global Surveyor (MGS) topography and MGS and Mars Odyssey (MO) gravity data, and applying a flexural model, it was shown that models of the lithospheric structure of Isidis Planitia are constrained by faulting at Nili Fossae to the northwest of the basin and, to a minor extent, at Amenthes Fossae to the southeast [9]. This suggests that a complex tectonic scenario should be included in explanations of Isidis's floor tilt.

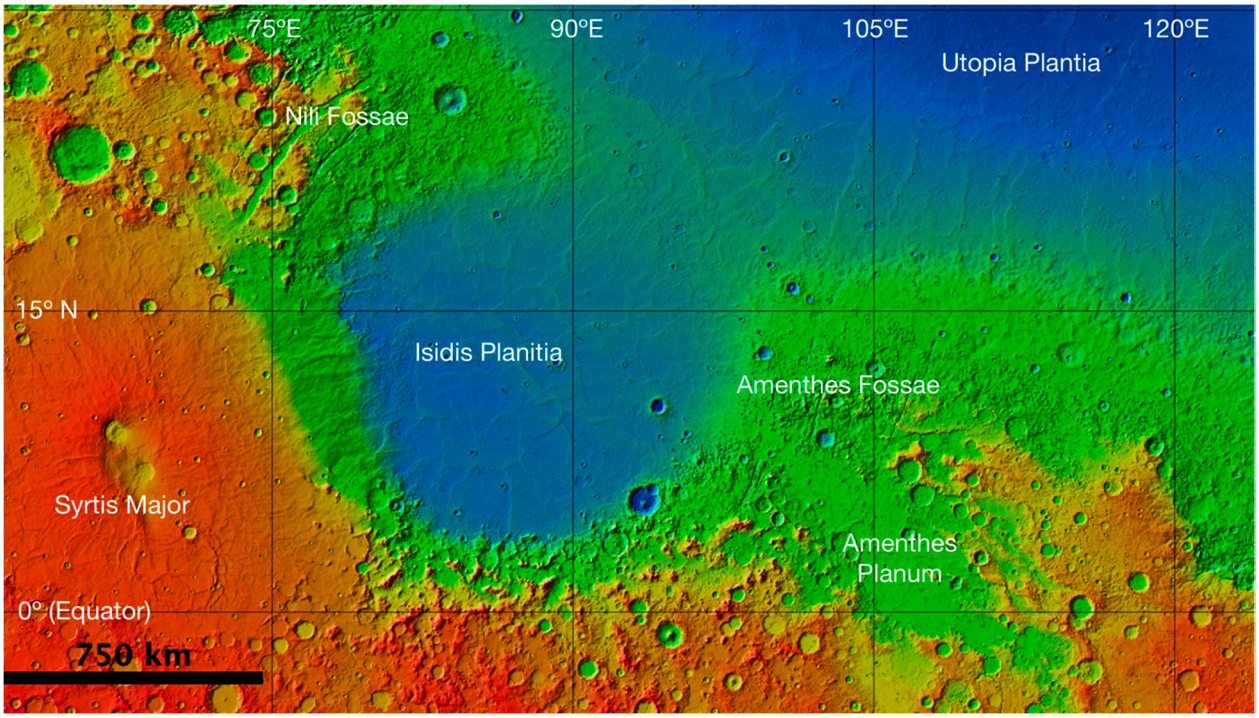

Figure 1. Context geomorphological map of the study area. Colors indicate elevations, with blue hues representing lowlands and yellow-red hues representing highlands. Isidis Planitia is center-left in the figure. The nomenclature and locations of Utopia Planitia, Amenthes Fossae, Amenthes Planum, Syrtis Major and Nili Fossae are also shown.

Geophysical data (e.g., [3,10–13]) have been collected globally on Mars, including over Isidis Planitia, but conclusive evidence of the geotectonic record hidden at depth has not yet been shown. The morphology and topography of an area reflect its surface evolution, overprinted on the attenuated surface expression of deep structures. A high-pass filter applied to the topography of Isidis Planitia [14] allowed the detection of the location and orientation of ridges (interpreted as wrinkle ridges), which had been

invisible to earlier surveys, because they were buried under the surface geological units. In this paper we present the results of our analysis of available MGS Mars Orbiter Laser Altimeter (MOLA) elevation data, and apply the measured *vs.* predicted depths diagram (MPD) technique [15] to the morphometric data of impact craters in Isidis Planitia. From our analysis we infer that the basement of Isidis Planitia is faulted, and suggest the approximate location where we predict the major fault system to exist. After describing the surface geology of the study area (Section 2), we summarize the geophysical techniques employed to study Isidis Planitia to date (Section 3). We then briefly describe our methods for data collection and processing (Section 4), followed by the presentation and discussion of our results (Sections 5 and 6).

2. Surface Geology of Isidis Planitia

Isidis is a very large basin, 1352 km in diameter [16], centered at approximately 87° E and 13° N. The latest estimate of the age of formation of this basin [17] is 3.95 Ga (+0.03/−0.04), based on Hartmann chronology [18], or 3.99 Ga (+0.02/−0.03), based on Neukum chronology [19]. The subsequent long and varied geological history of the region was subdivided [20] into several distinct phases: a Noachian impact-dominated phase, with subordinate volcanic and fluvioglacial activity; a volcanic-dominated episode at ~3.8–3.5 Ga, followed by fluvioglacial processes between 3.5 and 2.8 Ga; an aeolian-dominated phase, lasting to the present. Major resurfacing of the basin occurred during the acme of fluvioglacial activity, between ~3.4 and 3.1 Ga.

Because of the high density of valley networks along the basin southern rim [21], and its correspondence with two putative paleoshorelines, namely the Arabia and Deuteronilus contacts (e.g., [22]), Isidis Planitia was selected as the landing site for the Mars Express lander Beagle 2 [23]. New evidence for long-term water-related activity and climatic changes based on recent higher resolution datasets has led to a reappraisal of Isidis Planitia as a site for future landing missions [24]. Morphologies along the Deuteronilus paleoshoreline in south Isidis Planitia suggest that in the Late Hesperian/Early Amazonian a frozen sea existed in the basin, with the ice eventually melting and sublimating, leaving traces of past subglacial erosion and deposition on the floor of Isidis Planitia [25–27].

In the geological map [4] of the Martian northern plains based on Viking Orbiter MDIM 2.0, MGS MOLA DEM and Mars Orbiter Camera (MOC) wide and narrow angle imagery, and MO Thermal Emission Imaging System (THEMIS) infrared data, the unit covering the floor of Isidis Planitia is indicated as *AIi* which, together with the Early to Late Hesperian Syrtis Major Planum unit (*HIs*) and the Early Hesperian Amenthes Planum unit (*HIa*), forms the stratigraphy of the Isidis Province. Unit *AIi* correlates with the Vastitas Borealis formation. The unit consists of plain-forming material combining the characteristics of the Early Amazonian units ABv_i (Vastitas Borealis interior unit) and ABv_m (Vastitas Borealis marginal unit), that form the thin cover of Utopia Planitia to the north of Isidis. Trough features characterize the unit along its western margin, while the rest of the unit shows ridges of pitted cones interpreted as moraine-like debris [28]. A revision of the ages and extents of the units in Isidis Planitia and surrounding provinces is published in the recent global map of Mars [5] based on MOLA DEM and THEMIS infrared data complemented by higher resolution THEMIS visual and Mars Reconnaissance Orbiter (MRO) Context Camera (CTX) imagery where available, and by auxiliary published geological reconstructions ([5], and references therein) based on high resolution data from all recent missions to

Mars. The unit covering the floor of Isidis Planitia is identified as Late Hesperian lowland unit *lHl* (Figure 2), which is the same covering all of Vastitas Borealis. It is bounded to the north and northwest by the Late Hesperian transition unit *lHt*, to the east by the Early Hesperian transition unit *eHt* and a small sliver of Hesperian-Noachian transition unit *HNt*, and by the Middle Noachian highland unit *mNh* and massif unit *mNhm* to the south, while the Early Hesperian volcanic unit *eHv* bounds it to the southwest. Unit *lHl* marks the end of large-scale sedimentation in the lowland plains, and comprises deposits of various origin, including highland debris transported by fluvial activity, mass wasting, volcanism, and aeolian activity products. It is underlain by volcanic and volcaniclastic rocks. Similarly to Utopia Planitia, in Isidis Planitia unit *lHl* was modified by tectonism related to the weight of the deposits, which caused the formation of wrinkle ridges. Moderate tectonic activity continued into the Early Amazonian.

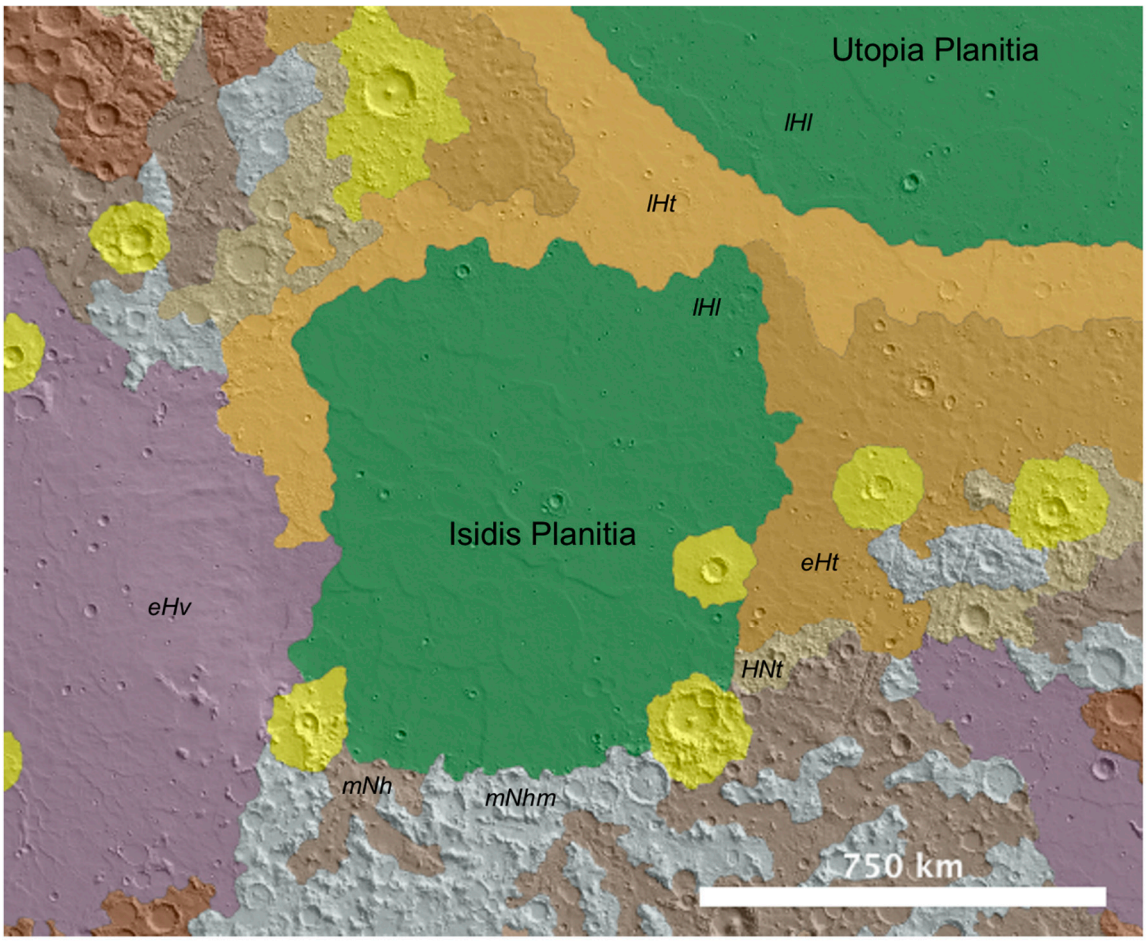

Figure 2. Geological map of Isidis Planitia and surrounding areas, constructed from shapefiles from [5] overlain on a MOLA shaded relief map, using Java Mission-planning and Analysis for Remote Sensing (JMARS). Unit symbols are explained in the text. Yellow units are Amazonian and Hesperian impact units (*AHi*).

The western section of the planitia's floor grades into knobby terrains, likely formed by wasting of the rocks cropping out at Syrtis Major Planum, as well as of Noachian highlands material [29]. The central and eastern sections of the basin appear smoother, and broadly similar to the Amenthes Planum terrains east of Isidis.

Complex impact craters in Isidis Planitia display lobate aprons, likely owing to the fluidization of ground-ice at the time of impact. The simple to complex impact crater transition here was determined to occur at a diameter of approximately ~12 km [30], much higher than the global Martian transition diameter of ~7 km [31]. This has been interpreted as evidence that the material forming the floor of Isidis basin on which the deep simple craters are observed is rheologically strong [30], possibly consisting of olivine-rich lava of Noachian and Hesperian age [32], an interpretation consistent with high values of thermal inertia observed in the southern half of the Isidis crater (Figure 3).

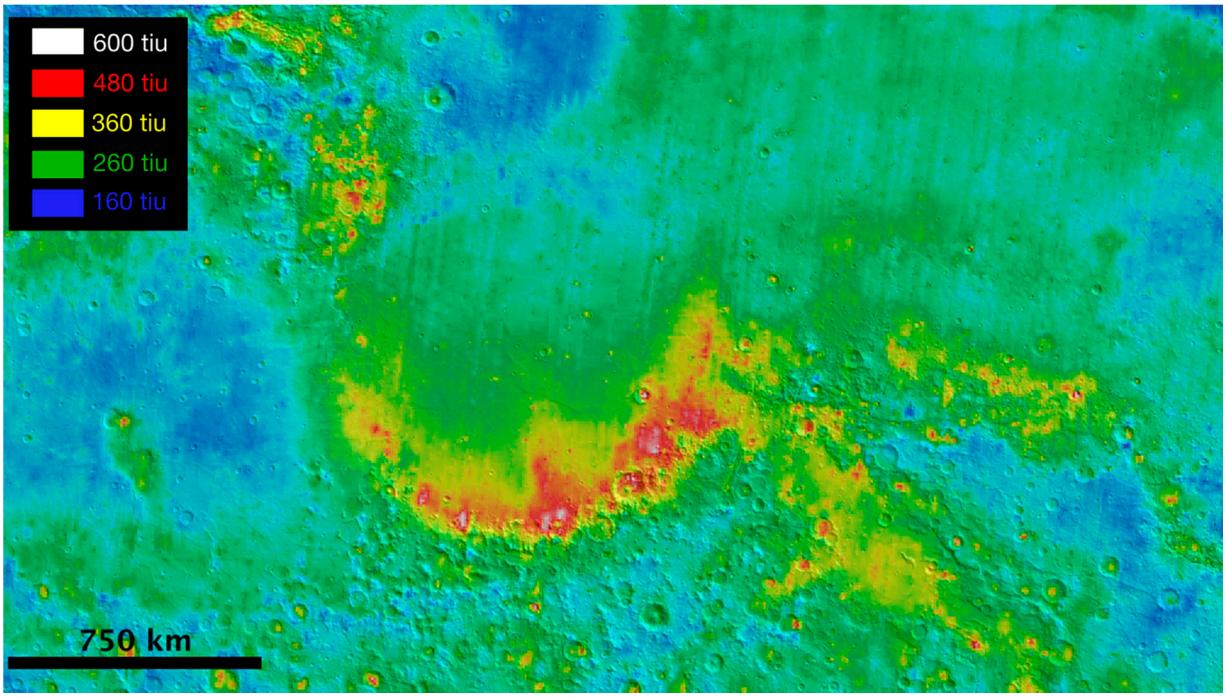

Figure 3. Variation of thermal inertia values adapted from [33]. Thermal inertia units are given as tiu (1 tiu = 1 J m^{-2} K^{-1} $s^{-1/2}$) and are only approximately representative of the average pixel value for the colors shown. The highest values of thermal inertia are observed in the southern portion of Isidis Planitia and, more moderately, in the NW-SE belt comprising the Nili and Amenthes areas, respectively NW and SE of the basin.

Apart from the dichotomy boundary, whose NW-SE trending scarp is interrupted by Isidis Planitia, the most prominent tectonic features in the region are represented by large grabens known as Nili Fossae, located northwest of the Isidis basin rim and broadly striking in a NE-SW direction, and those known as Amenthes Fossae, to Isidis's east. These grabens have been interpreted to be mid-Noachian, younger than the Isidis basin [4].

3. Geophysical Research in Isidis Planitia

Early Viking Orbiter 2 geophysical data collected over the large topographic depression in Isidis Planitia indicate this to be the location of a prominent positive gravity anomaly [34]. This was interpreted as a mass concentration (*mascon*) suggesting an uplift of the crust-mantle boundary resulting from a large impact cratering event. Subsequent observations acquired by the radio science experiment on-board MGS, used to produce a global high-resolution gravitational field model [10,12], determined a positive

anomaly value of 600 mgal for Isidis Planitia. This is the largest impact-associated gravity anomaly on Mars, surpassed only by the gravity anomalies measured in connection with the major young volcanic provinces (Olympus and Tharsis Montes). Isidis Planitia's positive anomaly is surrounded by a broad negative anomaly annulus, possibly produced by a combination of flexural response of the lithosphere to loads or uncompensated crustal thickening caused by the impact [10].

Using MGS MOLA and gravity from Doppler tracking, [11] calculated global Bouguer gravity anomalies, interpreting the data assuming the anomalies were caused by thickness variation of a crust of uniform density equal to 2900 km m^{-3}. The resulting average crustal thickness was 50 km, with the lowest value of 3 km located under Isidis Planitia. Further refinement of gravity models [35,36] confirmed the large positive anomaly in Isidis Planitia. Based on these models, and assuming a crust-mantle density contrast of 600 kg m^{-3}, Isidis Planitia's minimum crustal thickness was recalculated to be 5.8 km [37], most of which (~5 km) possibly formed by post-basin infilling principally by high density volcanic material from Syrtis Major. A corollary of these gravity models is that the impact that formed Isidis basin created a transient cavity intercepting the mantle, which would have then isostatically rebounded.

The floor of Isidis basin slopes southwest at an angle of ~0.02°, in contrast with the global south to north slope of ~0.036°. This indicates that subsequent tectonic evolution took place after the impact basin formation, possibly connected with the Syrtis Major volcanic province to the west [7], with the presence of a body of water in Isidis, or with sediment load in Utopia Planitia to the northeast. A flexural model of the crust tested these last two scenarios [8], finding that a 12 km load of sediments in Utopia centered 800 km away from Isidis would result in a peripheral bulge between Utopia and Isidis, causing the observed slope. Subsequently [9] studied the lithospheric structure and tectonics using gravity and topography data for crustal inversion, and then applying a flexural model of the crust, including bending and membrane stresses, to reproduce the tectonic features observed around Isidis. These results imply that the basin fill has densities higher than the crustal density. The layer of sediments covering the basin floor must therefore be relatively thin, above a much thicker sequence of lava flows. The model also constrains the thickness of the elastic lithosphere to be between 100 km and 180 km, and the heat flux to range between 13.6 mW m^{-2} and 26 mW m^{-2} at the time of loading.

Two subsurface sounding radars, the Mars Express Mars Advanced Radar for Subsurface and Ionosphere Sounding (MARSIS; [38]) and the MRO Shallow Subsurface Radar (SHARAD; [39]), probed the first few tens to hundreds of meters of Isidis's subsurface. The data did not provide sufficient evidence of density or compositional layering in this region [40]. This could be caused by insufficient vertical resolution of the techniques as they are applied to lithic materials (~50 m for MARSIS and ~5 m for SHARAD), or could be due to a strong attenuation in the subsurface, as would happen in dense volcanic rocks. In the latter case, the maximum possible depth of detection for SHARAD would be of the order of a few hundred meters, while for MARSIS it would increase to several hundred meters [13], corroborating geophysical models that invoke the presence of dense volcanic rocks at these depths.

4. Data and Methods

To analyse the topography of Isidis Planitia we used the 128 pixel/degree (463 m/pixel) resolution MGS MOLA Mission Experiment Gridded Data Record (MEGDR) obtained from the Geosciences Node of NASA's Planetary Data System (PDS) archive at Washington University in St. Louis

(http://pds-geoscience.wustl.edu/missions/mgs/megdr.html). While we do not discuss geomorphological features in this work, we visually explored the study area using MO THEMIS daytime and nighttime infrared 100 m/pixel resolution data and MRO CTX panchromatic images (resolution: ~6 m/pixel). We mapped and conducted morphometric analysis of the data using the commercial software ArcGIS version 10.2.1, the open source software Quantum GIS (QGIS) version 2.2.0 (Valmiera), and the on-line GIS application JMARS (Java Mission-planning and Analysis for Remote Sensing) from Arizona State University (http://jmars.asu.edu), applying an equidistant cylindrical projection over a Mars IAU 2000 spheroid of equatorial radius = 3,396,190 m.

To gain insight into the geological processes that modified the basin morphology, we explored the distribution of MOLA MEGDR measured depths (d) and diameters (D) of impact craters in Isidis Planitia by applying known d/D power laws, representing the statistical behavior of impact crater dimensions on Mars. Impact craters from a published database of craters of diameter $D \geq 1$ km [41] completely contained within Isidis Planitia were selected. From the impact crater diameters, theoretical (pre-modification fresh crater) depths were calculated using power laws [42] for impact craters comprised between −40°N and +40°N latitude: $d = 0.084\ D^{1.245}$ (simple); $d = 0.229\ D^{0.567}$ (complex). These predicted values of depth were used as proxies of the crater diameters and plotted on the horizontal axis of a Cartesian diagram, with the measured depths (from [41]) plotted on the vertical axis, following the procedure described in [15]. This measured depths *vs.* predicted depths diagram is henceforward referred to as MPD. Young (fresh) and older unmodified craters are immediately identified in the MPD by the fact that their data points plot along an approximately 1:1 trend, since their measured depths are close to the theoretical values of depth calculated by the d/D power laws [15]. Data points representative of impact craters that have been modified by geological processes are readily identified in the MPD, because they plot away from the unmodified craters 1:1 trend.

The MOLA shot-point data from which the gridded elevation raster is produced are unevenly distributed latitudinally, meaning that the likelihood of the laser shots missing small craters is especially high at subequatorial latitudes [15]. The smoothing effect of the interpolation producing the MEGDR dataset can distort or even mask smaller morphological features, being particularly pronounced for the 128 pixel/degree digital elevation model (DEM) at sub-equatorial latitudes, where only 31% of the pixels of the DEM contain actual elevation values [43]. In addition, given the dimensions of small craters relative to the nominal along-track footprint spacing of ~300–400 m, the laser signal is unlikely to return exactly from the deepest part of the crater floor or from its rim [44]. The resulting uncertainty of the measurement of elevations of rims and floors of impact craters in the database used [41], and, hence, the error of the crater depths measured from the MOLA MEGDR dataset, has been quantified to be ±25 m at the Equator [41].

5. Results

A total of 148 impact craters located inside of the −3600 m MOLA elevation contour line enclosing the Isidis basin (Figure 4) were analysed and interpreted. The isoline approximates the inner rim shape of the basin. Further inside Isidis Planitia, the contour lines corresponding to elevations of −3700 m, −3800 m and −3900 m are not concentric to the outer −3600 m isoline. Instead, the −3700 m and −3800 m contour lines run across the center of the basin along a roughly straight NW-SE direction, and mimic the rim of the basin only in its southwestern sector, where all isolines are parallel and close to each other,

indicating steep slopes. The −3900 m contour line is fully enveloped by the −3800 m contour, and limited to the SW sector of Isidis Planitia, which is the deepest portion of the basin. We subdivided the impact craters into three groups: those located at higher elevations than −3700 m, in the northeastern sector of the basin (downward triangles in Figure 4); those located in a central belt striking NW-SE, between the straight sections of the −3700 m and −3800 m contour lines (triangles in Figure 4); and those at the lowest elevations in the southwestern sector (circles in Figure 4).

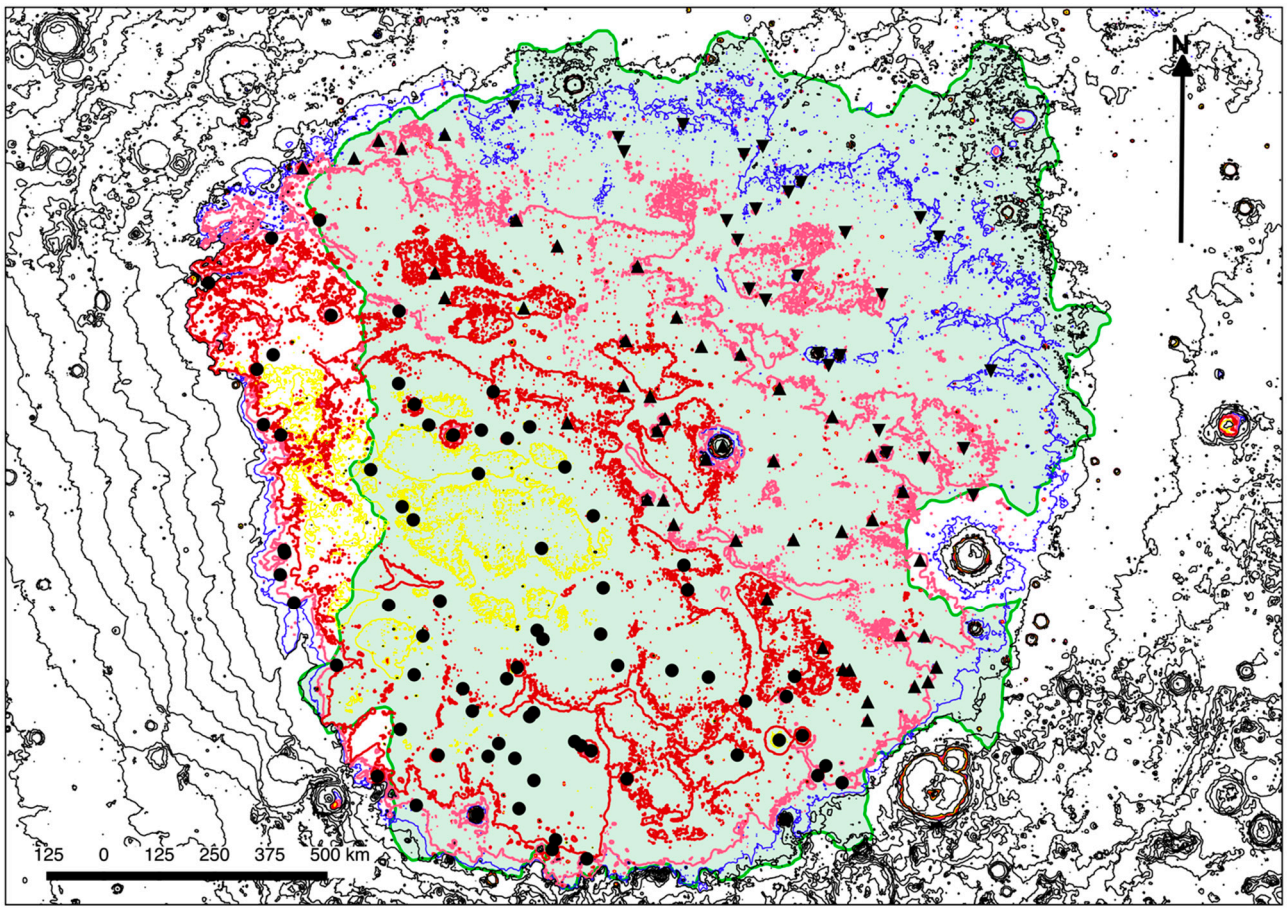

Figure 4. Geographical distribution of impact craters (black symbols). North is indicated by the arrow. The extent of unit *lHl*, represented by the light green polygon, is shown for reference. The topography of the region is indicated by contour lines calculated from MOLA MEGDR, with a contour interval of 500 m. In the interior of Isidis Planitia the isolines corresponding to elevations of −3600 m (blue), −3700 m (pink), −3800 m (red) and −3900 m (yellow) are shown. In the center of the basin the −3800 m and −3700 m contour lines run almost linearly and parallel to a NE-SW direction. These sections of the contour lines were used to subdivide the impact craters into three sectors: northeast (between −3600 m and −3700 m elevation), center (between −3700 m and −3800 m), and southwest (elevations lower than −3800 m). The impact crater symbols are circles (southwestern sector of Isidis basin), triangles (central sector), and downward triangles (northeastern sector), consistent with the shape of the data points in the diagram of Figure 5.

The MPD is shown in Figure 5, where it can be observed that the data points are distributed along two separate trends: the first, comprising the majority of the craters, approximately corresponds to the 1:1 line (dashed line in Figure 5), which is the baseline representing fresh impact craters [15]. The craters plotting along this trend have not undergone significant morphological modification since their formation. Craters located in all studied sectors in Isidis Planitia belong to this group. The best fit model for these craters is described by the linear equation: $y = 1.129x + 0.0605$ ($R^2 = 0.7049$); slightly steeper than the baseline. This indicates material harder than the average lithologies on which the power laws used to calculate the predicted values are based [15,45].

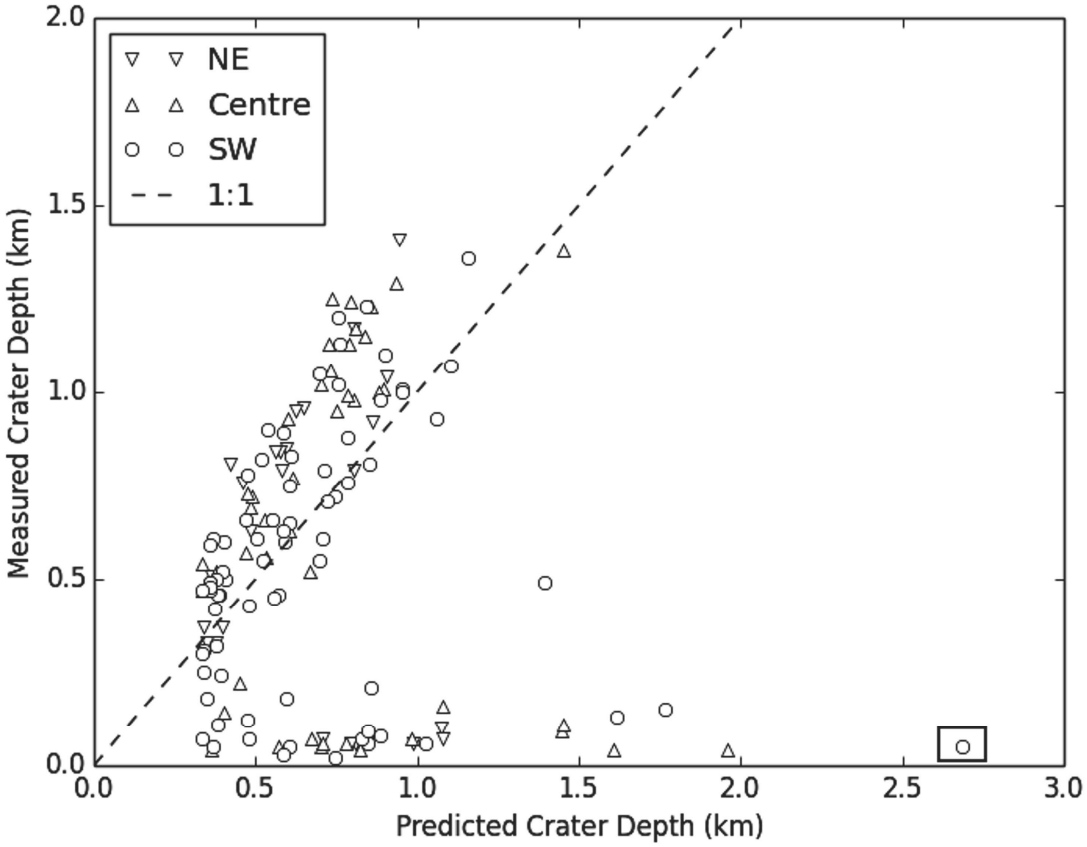

Figure 5. Measured depth *vs.* predicted depth diagram (MPD) of impact craters in Isidis Planitia. The dashed line is the 1:1 line (baseline), representing fresh craters. Symbols differ depending on whether the craters are located in the northeastern sector of Isidis Planitia (downward triangles), in the center (triangles), or in the southwestern sector (circles). The size of the data point symbols includes an estimated error of ±25 m of the measured depths (refer to Section 4). Most craters from all three locations are plotted along or very close to the baseline. Of those craters plotting close to the horizontal axis, the majority are from the central and southwestern sections of Isidis Planitia. The data point enclosed in the square (*x*-*y* coordinates: 2.68, 0.05) corresponds to a feature designated as 13-000037 in [41]'s database. The diagram and its interpretation are discussed in the text.

The second group, comprising the data points representing 40 impact craters, generally plots along a trend quasi-parallel (almost coincident) to the horizontal axis of the diagram and, with the exception of only four data points (downward triangles), it represents craters in the central (triangles) and southwestern

(circles) sectors of Isidis Planitia. This group includes crater 13-000037 [41], which has a rating of 2 in [41]'s confidence scale for crater identification, meaning a 50% chance that this feature is not an impact crater. We excluded this data point from interpretation noting, however, that the flat MPD trend described by the craters in this group remains. This horizontal trend cannot be reconciled with a process of steady and continuous degradation of the morphologies of the corresponding impact craters, which would be represented by linear trends parallel to the baseline, whose distance from the 1:1 line increases with the period of time that the craters have been exposed to modification (for theoretical explanation see [15]). Instead, the dramatic displacement of these data points from the baseline indicates that the dimensions of these craters have been modified by a fast geological process occurring mostly in the central and southwestern sectors of Isidis Planitia.

Some of the craters belonging to this group have been discussed in previous studies and defined as "stealth" (e.g., [14,46,47]) or "type 2" craters [48]. Stealth craters are characterized by subdued topographies, with smooth, shallow floors, no ejecta apron and no ridge associated with their rims, and are found scattered all over the northern plains. Stealth craters differ from all other types of Martian impact craters, because their depths are typically <300 m, regardless of their sizes: their dimensions do not conform to any *depth*/*Diameter* power law. A number of processes have been proposed to explain the unique morphologic and morphometric characteristics of stealth craters: erosion and deposition due to outflow channel processes; impact into water; glacial obliteration; accelerated sedimentation in water bodies; redistribution of sediments by wind [14]. Flooding by volcanic flows, similarly to the interpretation of lunar ghost craters, has also been proposed [48], as well as differential compaction of sedimentary covers [47]. Each of these mechanisms focuses on the surface processes producing the peculiar morphologic and morphometric characteristics of the craters. Irrespective of the specific process advocated, the features have always been interpreted as having formed as real impact craters, subsequently modified, eroded and infilled. We therefore interpret the quasi-horizontal alignment of these craters in the MPD as evidence of loss of depth by infilling, with craters once fresh (plotting close to the 1:1 line) quickly filled, so that their measured depths have become almost negligible. In our discussion of these craters (Section 6), we focus on the relationship between their geographic distribution and the topography of the Isidis basin, interpreting this evidence in a tectonic context.

6. Discussion and Conclusions

In the previous sections we showed that: (1) the −3700 m and −3800 m contour lines are not concentric to the shape of the basin, but follow an almost parallel and linear (to a large degree of approximation) NW-SE direction in the center of Isidis Planitia; (2) the southwestern sector of Isidis Planitia is topographically the most depressed area in the basin (see also [20]); (3) in the MPD the impact craters plotting along a quasi-horizontal line intercepting the y-axis at a value ~0 are located in the central and southwestern sectors of the basin.

With regards to (1) we observe that straight and parallel contour lines are diagnostic of the topography of fault planes, which typically disrupt existing morphologies. Therefore, even though no fault plane is observable in the imagery, we interpret the approximately straight sections of the −3700 m and −3800 m elevation isolines as fault lines, marking the (subdued) traces of one or more fault systems striking NW-SE. This interpretation is consistent with evidence (2), further indicating that the largest vertical displacement is

measured in the southwestern sector of the basin. This, in turn, implies that the putative fault planes dip SW. This faulted basement scenario explains observation (3), because some of the impact craters in the central and southwestern sectors of Isidis Planitia would have been downthrown together with the basement on which they rested, and subsequently would have been infilled almost completely. Most coeval impact craters located NE would have only experienced limited infilling, being located at higher elevations. In the MPD the data points plotting close to the baseline represent a majority of impact craters emplaced after the floor of Isidis Planitia assumed its present topography.

A minimum value of vertical displacement can be estimated by evaluating the degree of infilling of the impact craters plotting parallel to the horizontal axis of the MPD (Figure 5). If we assume that the crater dimensions were uniquely modified by infilling, then depth losses of ~1–2 km can be estimated by the positions of the data points. Assuming that the craters were selectively infilled because of being located in topographic depressions produced by the faulting system, the degree of infilling should provide an estimate of the vertical displacement along the fault planes of ~1–2 km. Normal faults causing these vertical displacements are not unreasonable on Mars, especially given the overall linear extent of the fault system (almost the entire inner diameter of Isidis Planitia, for the −3800 m contour line). The estimated vertical displacement represents the last "measured" value: we cannot exclude (and, in fact, we consider this to be the most likely scenario) that the basement faulting occurred over an extended period of time; hence, older craters laying on the basement would have been totally infilled and their topographic expression completely lost, while younger craters were still forming on the downthrown surface. In both cases, a "measurable" vertical displacement of ~1–2 km indicates that the fault planes reach deep into the lithosphere (e.g., [49]).

Because the crust in Isidis Planitia is extremely thin, we speculate that our putative fault planes will extend deeply enough to cross the crust-mantle boundary under Isidis Planitia. This implies that the upper mantle at these depths must behave brittlely, which is the case if the lithosphere is capable of sustaining high strain rates, the geothermal gradient is low, or for a combination of both factors. A cold and/or hard lithosphere is consistent with reconstructions of the Isidis impact event completely stripping the crustal material from the impacted site, and subsequent deposition of voluminous and thick layers of high-density volcanic material in the basin cavity [37]. Our data and interpretation do not allow us to speculate further whether the source of the volcanic material was Syrtis Major, although this appears likely, given the proximity of this volcanic province to Isidis Planitia, and particularly to its SW sector. In this case, the tectonic activity associated with the fault system should have started at the latest in the Early Hesperian, which is the age of Syrtis Major volcanics. We are unable at this stage to conclusively determine whether the fault system was in any way related to the volcanic activity, for example by coeval loading of the volcanic construct or of the infilling material. However, given the general NW-SE orientation of Amenthes Planum and its location relative to the −3800 m and −3700 m isolines in Isidis Planitia, we speculate that there may exist a tectonic correlation between the formation of Amenthes Planum and the putative fault system under the present-day floor of the Isidis basin. The nature and extent of this correlation will require further investigation.

Current geotectonic interpretations of the evolution of the Martian eastern hemisphere have been based on visible structures. In relation to the Isidis-Syrtis center of tectonic activity, 2271 compressional structures (ridges), mostly of Hesperian age, and 160 younger extensional structures (grabens) were mapped [50]. The dominance of surface compressional structures in the Martian eastern hemisphere has

influenced models of its geotectonic evolution. The identification and interpretation of tectonic structures at depth by a reinterpretation of the geophysical data already available, or by new geophysical surveys of the Martian subsurface might, however, lead to a significant review of current lithospheric models. The approach we presented in this paper could be applied to other regions, and could be useful as a tool to spatially and temporally narrow areas and techniques for future high-resolution geophysical studies.

Acknowledgments

Graziella Caprarelli acknowledges infrastructural and funding support for this research from the University of South Australia. The authors are grateful to all the teams and individual researchers who made available to the scientific community the Martian datasets used in this work. Graziella Caprarelli acknowledges Stuart J. Robbins and James A. Skinner Jr., for their prompt replies to requests of clarification on the impact crater database and the Mars global map, respectively. An earlier version of this manuscript was critiqued by two anonymous reviewers, whose insightful comments greatly helped to improve the paper.

Author Contributions

Graziella Caprarelli conceived of the work, collected and interpreted the data, prepared the figures and wrote the manuscript. Roberto Orosei advised on the scientific content of the paper, researched and summarized the geophysical studies of Isidis Planitia and contributed to writing Section 3.

Conflicts of Interest

The authors declare no conflict of interest.

References

1. Wichman, R.W.; Schultz, P.H. Sequence and mechanisms of deformation around the Hellas and Isidis impact basins on Mars. *J. Geophys. Res.* **1989**, *94*, 17333–17357.
2. Frey, H.; Sakimoto, S.; Roark, J. MOLA topographic structure of the Isidis and Utopia impact basins. In Proceedings of the 30th Lunar and Planetary Science Conference, Houston, TX, USA, 15–29 March 1999.
3. Smith, D.E.; Zuber, M.T.; Solomon, S.C.; Phillips, R.J.; Head, J.H.; Garvin, J.B.; Banerdt, W.B.; Muhleman, D.O.; Pettengill, G.H.; Neumann, G.A.; *et al.* The global topography of Mars and implications for surface evolution. *Science* **1999**, *284*, 1495–1503.
4. Tanaka, K.; Skinner, J.; Hare, T. G*eologic Map of the Northern Plains of Mars*; USGS Scientific Investigations Maps 2888; USGS: Reston, VA, USA, 2005; scale 1:15,000,000.
5. Tanaka, K.L.; Skinner, J.A.; Dohm, J.M.; Irwin, R.P., III; Kolb, E.J.; Fortezzo, C.M.; Platz, T.; Michael, G.G.; Hare, T. *Geologic Map of Mars*; USGS Scientific Investigations Maps 3292; USGS: Reston, VA, USA, 2014; scale 1:20,000,000.
6. Orosei, R.; Bianchi, R.; Coradini, A.; Espinasse, S.; Federico, C.; Ferriccioni, A.; Gavrishin, A.I. Self affine behavior of Martian topography at kilometre scale from Mars Orbiter Laser Altimeter data. *J. Geophys. Res.* **2003**, *108*, doi:10.1029/2002JE001883.

7. Hiesinger, H.; Head, J.W., III. The Isidis Basin of Mars: New results from MOLA, MOC, and Themis. In Proceedings of the 35th Lunar and Planetary Science Conference, Houston, TX, USA, 15–19 March 2004.
8. McGowan, E.M.; McGill, G.E. Anomalous tilt of Isidis Planitia, Mars. *Geophys. Res. Lett.* **2006**, *33*, L08S06.
9. Ritzer, J.A.; Hauk, S.A., II. Lithospheric structure and tectonics at Isidis Planitia, Mars. *Icarus* **2009**, *201*, 528–539.
10. Smith, D.E.; Sjogren, W.L.; Tyler, G.L.; Balmino, G.; Lemoine, F.G.; Konopliv, A.S. The gravity field of Mars: Results from Mars Global Surveyor. *Science* **1999**, *286*, 94–97.
11. Zuber, M.T.; Solomon, S.C.; Phillips, R.J.; Smith, D.E.; Tyler, G.L.; Aharonson, O.; Balmino, G.; Banerdt, W.B.; Head, J.W.; Johnson, C.L.; *et al.* Internal structure and early thermal evolution of Mars from Mars Global Surveyor topography and gravity. *Science* **2000**, *287*, 1788–1793.
12. Tyler, G.L.; Balmino, G.; Hinson, D.P.; Sjogren, W.L.; Smith, D.E.; Simpson, R.A.; Asmar, S.W.; Priest, P.; Twicken, J.D. Radio science observations with Mars Global Surveyor: Orbit insertion through one Mars year in mapping orbit. *J. Geophys. Res.* **2001**, *106*, 23327–23348.
13. Orosei, R.; Jordan, R.L.; Morgan, D.D.; Cartacci, M.; Cicchetti, A.; Duru, F.; Gurnett, D.A.; Heggy, E.; Kirchner, D.L.; Noschese, R.; *et al.* Mars Advanced Radar for Subsurface and Ionospheric Sounding (MARSIS) after nine years of operation: A summary. *Planet Space Sci.* **2014**, doi:10.1016/j.pss.2014.07.010.
14. Head, J.W., III; Kreslavsky, M.A.; Pratt, S. Northern lowlands of Mars: Evidence for widespread volcanic flooding and tectonic deformation in the Hesperian Period. *J. Geophys. Res.* **2002**, *107*, doi:10.1029/2000JE001445.
15. Caprarelli, G. Introducing and discussing a novel diagrammatic representation of impact crater dimensions. *Icarus* **2014**, *237*, 366–376.
16. Frey, H. Ages of very large impact basins on Mars: Implications for the late heavy bombardment in the inner solar system. *Geophys. Res. Lett.* **2008**, *35*, L13203.
17. Robbins, S.J.; Hynek, B.M.; Lillis, R.J.; Bottke, W.F. Large impact crater histories of Mars: The effect of different model crater age techniques. *Icarus* **2013**, *225*, 173–184.
18. Hartmann, W.K. Martian cratering 8: Isochron refinement and the chronology of Mars. *Icarus* **2005**, *174*, 294–320.
19. Ivanov, B.A. Mars/Moon cratering rate ratio estimates. *Chronol. Evol. Mars* **2001**, *96*, 87–104.
20. Ivanov, M.A.; Hiesinger, H.; Erkeling, G.; Hielscher, F.J.; Reiss, D. Major episodes of geologic history of Isidis Planitia on Mars. *Icarus* **2012**, *218*, 24–46.
21. Crumpler, L.S.; Tanaka, K.L. Geology and MER target site characteristics along the southern rim of Isidis Planitia, Mars. J. *Geophys. Res*. **2003**, *108*, doi:10.1029/2002JE002040.
22. Clifford, S.M.; Parker, T.J. The evolution of the Martian hydrosphere: Implications for the fate of a primordial ocean and the current state of the Northern Plains. *Icarus* **2001**, *154*, 40–70.
23. Bridges, J.C.; Seabrook, A.M.; Rothery, D.A.; Kim, J.R.; Pillinger, C.T.; Sims, M.R.; Golombek, M.P.; Duxbury, T.; Head, J.H.; Haldemann, A.F.C.; *et al.* Selection of the landing site in Isidis Planitia of Mars probe Beagle 2. *J. Geophys. Res*. **2003**, *108*, doi:10.1029/2001JE001820.

24. Erkeling, G.; Reiss, D.; Hiesinger, H.; Poulet, F.; Carter, J.; Ivanov, M.A.; Jaumann, R.; Tirsch, D.; Raack, J.; Ruesch, O. Southern Isidis Planitia. In Proceedings of the ExoMars 2018 First Landing Site Selection Workshop, Villanueva de la Cañada, Spain, 26–28 March 2014.
25. Erkeling, G.; Reiss, D.; Hiesinger, H.; Poulet, F.; Carter, J.; Ivanov, M.A.; Hauber, E.; Jaumann, R. Valleys, paleolakes and possible shorelines at the Libya Montes/Isidis boundary: Implications for the hydrologic evolution of Mars. *Icarus* **2012**, *219*, 393–413.
26. Erkeling, G.; Reiss, D.; Hiesinger, H.; Ivanov, M.A.; Hauber, E.; Bernhardt, H. Landscape formation at the Deuteronilus contact in southern Isidis Planitia, Mars: Implications for an Isidis Sea? *Icarus* **2014**, *242*, 329–351.
27. Guidat, T.; Pochat, S.; Bourgeois, O.; Souček, O. Landform assemblage in Isidis Planitia, Mars: Evidence for a 3 Ga old polythermal ice sheet. *Earth Planet. Sci. Lett*. **2015**, *411*, 253–267.
28. Grizzaffi, P.; Schultz, P.H. Isidis Basin: Site of ancient volatile-rich layer. *Icarus* **1989**, *77*, 358–381.
29. Ivanov, M.A.; Head, J.W., III. Syrtis Major and Isidis Basin contact: Morphological and topographic characteristics of Syrtis Major lava flows and material of the Vastitas Borealis Formation. *J. Geophys. Res.* **2003**, *108*, doi:10.1029/2002JE001994.
30. Boyce, J.M.; Mouginis-Mark, P.; Garbeil, H.; Tornabene, L. Deep impact craters in the Isidis and southwestern Utopia Planitia regions of Mars: High target material strength as a possible cause. *Geophys. Res. Lett.* **2006**, *33*, L06202.
31. Garvin, J.B.; Sakimoto, S.E.H.; Frawley, J.J. Craters on Mars: Global geometric properties from gridded MOLA Topography. In Proceedings of the Sixth International Conference on Mars, Pasadena, CA, USA, 20–25 July 2003.
32. Tornabene, L.L.; Moersch, J.E.; McSween, H.Y., Jr.; Hamilton, V.E.; Piatek, J.L.; Christensen, P.R. Surface and crater-exposed lithologic units of the Isidis Basin as mapped by coanalysis of THEMIS and TES derived data products. *J. Geophys. Res.* **2008**, *113*, E10001.
33. Christensen, P.R.; Moore, H.J. The martian surface layer. In *Mars*; Kieffer, H.H., Jakosky, B.M., Snyder, C.W., Matthews, M.S., Eds.; University of Arizona Press: Tucson, AZ, USA, 1992; pp. 686–729.
34. Sjogren, W.L. Mars gravity—High-resolution results from Viking Orbiter 2. *Science* **1979**, *203*, 1006–1010.
35. Lemoine, F.G.; Smith, D.E.; Rowlands, D.D.; Zuber, M.T.; Neumann, G.A.; Chinn, D.S.; Pavlis, D.E. An improved solution of the gravity field of Mars (GMM-2B) from Mars Global Surveyor. *J. Geophys. Res.* **2001**, *106*, 23359–23376.
36. Yuan, D.-N.; Sjogren, W.L.; Konopliv, A.S.; Kucinskas, A.B. Gravity field of Mars: A 75th degree and order Model. *J. Geophys. Res.* **2001**, *106*, 23377–23402.
37. Neumann, G.A.; Zuber, M.T.; Wieczorek, M.A.; McGovern, P.J.; Lemoine, F.G.; Smith, D.E. Crustal structure of Mars from gravity and topography. *J. Geophys. Res. Planets* **2004**, *109*, E08002.
38. Picardi, G.; Biccari, D.; Seu, R.; Marinangeli, L.; Johnson, W.T.K.; Jordan, R.L.; Plaut, J.; Safaenili, A.; Gurnett, D.A.; Ori, G.G.; *et al.* Performance and surface scattering models for the Mars Advanced Radar for Subsurface and Ionosphere Sounding (MARSIS). *Planet. Space Sci*. **2004**, *52*, 149–156.

39. Seu, R.; Phillips, R.J.; Biccari, D.; Orosei, R.; Masdea, A.; Picardi, G.; Safaeinili, A.; Campbell, B.A.; Plaut, J.J.; Marinangeli, L.; *et al.* SHARAD sounding radar on the Mars Reconnaissance Orbiter. *J. Geophys. Res. Planets* **2007**, *112*, E05S05.
40. Heggy, E.; Boisson, J.; Clifford, S.M.; Plaut, J.J.; Ferro, A.; Gim, Y. Constraining the equatorial basin sedimentation chronology from MARSIS tomographic data analysis. In Proceedings of the American Geophysical Union Fall Meeting, San Francisco, CA, USA, 13–17 December 2010.
41. Robbins, S.J.; Hynek, B.M. A new global database of Mars impact craters ≥ 1 km: 1. Database creation, properties, and parameters. *J. Geophys. Res.* **2012**, *117*, E05004.
42. Robbins, S.J.; Hynek, B.M. A new global database of Mars impact craters ≥ 1 km: 2. Global crater properties and regional variations of the simple-to-complex transition diameter. *J. Geophys. Res.* **2012**, *117*, E06001.
43. Som, S.M.; Greenberg, H.M.; Montgomery, D.R. The Mars orbiter laser altimeter dataset: Limitations and improvements. *Mars* **2008**, *4*, 14–26.
44. Mouginis-Mark, P.J.; Garbeil, H.; Boyce, J.M.; Ui, C.S.E.; Baloga, S. Geometry of martian impact craters: First results from an interactive software package. *J. Geophys. Res*. **2004**, *109*, E08006.
45. Caprarelli, G.; Pondrelli, M.; Di Lorenzo, S.; Marinangeli, L.; Ori, G.G.; Greeley, R.; Neukum, G. A description of surface features in north Tyrrhena Terra, Mars: Evidence for extension and lava flooding. *Icarus* **2007**, *191*, 524–544.
46. Kreslavski, M.A.; Head, J.W., III. Stealth craters in the northern lowlands of Mars: Evidence for a buried Early-Hesperian-aged unit. In Proceedings of the 32nd Lunar and Planetary Science Conference, Houston, TX, USA, 12–16 March 2001.
47. Buczkowski, D.L. Stealth quasi-circular depressions (sQCDs) in the northern lowlands of Mars. *J. Geophys. Res.* **2007**, *112*, E09002.
48. Boyce, J.M.; Mouginis-Mark, P.; Garbeil, H. Ancient oceans in the northern lowlands of Mars: Evidence from impact crater depth/diameter relationships. *J. Geophys. Res.* **2005**, *110*, E03008.
49. Schultz, R.A.; Lin, J. Three-dimensional normal faulting models of the Valles Marineris, Mars, and geodynamic implications. *J. Geophys. Res.* **2001**, *106*, 16549–16566.
50. Anderson, R.C.; Dohm, J.M.; Haldemann, A.F.C.; Pounders, E.; Golombek, M.; Castano, A. Centers of tectonic activity in the eastern hemisphere of Mars. *Icarus* **2008**, *195*, 537–546.